UNIVERSITY OF CALIFORNIA SAN DIEGO

Passivation for Selective ALD and CVD of Metals, Metal Oxides, and Metal Silicides

A Thesis submitted in partial satisfaction of the requirements for the degree Master of Science

in

NanoEngineering

by

Ashay Anurag

Committee in charge:

Professor Andrew C. Kummel, Chair
Professor David Fenning
Professor Andrea Tao

2019

The Thesis of Ashay Anurag is approved, and it is acceptable in quality and form for publication on microfilm and electronically:

_____

_____

_____

Chair

University of California San Diego

2019

Table of Contents

List of Figures

Acknowledgements

The materialization and completion of this thesis would not have been possible without the kind support and help of many individuals and organizations. I would like to extend my sincere gratitude to all of them.

I would like to first recognize my advisor, Professor Andrew Kummel, who has been a very patient, direct, open, and readily available source of much knowledge and experience. He has provided many opportunities to develop myself into a motivated engineer by allowing me to present my work at several conferences. His guidance and direction has allowed me to complete this incredible journey.

My sincerest thanks to Michael Breeden for training me, providing his guidance, supervising me as well as for providing the necessary information regarding the project. He has spent many hours of his time helping with data discussion and analysis, as well as helping me prepare for weekly group meeting presentations and conference presentations. A large portion of this project wouldn't have been possible without the help, support and technical expertise of Scott Ueda, Victor Wang and Aaron Mcleod. They taught me a great deal about chamber maintenance, atomic force microscopy and were always available to answer all my questions.

This thesis would not have been possible without the tireless efforts of Dr. Jong Choi, Dr. Chris Ahles and Yunil Cho. Their patience, scientific acumen and strong work ethic have taught me a great deal, without their processes testing my samples, I would not have the data required for this thesis. They have also helped me understand theorized and in some way trained me to think like a successful graduate student.

Having spent a year in the Kummel Lab, I have had the pleasure to be in the company of many fascinating souls. I have worked with them day in, day out, and have got to know them outside of work. The memories in and out of lab with these people will never be forgotten and really made my time in San Diego a positive, enjoyable experience a special thanks to Victor Wong for that. I need to also thank

Francis Yu, a fellow colleague and friend that I have gotten to work with over a few month. He has been a valuable contributor to the Kummel lab. He is a great student, and I know that he will see his hard work continue to pay off in the future.

I want to thank my committee members for being involved in my Thesis defense presentation. My committee includes Professor David Fenning, and Professor Andrea Tao.

A special thanks to the Semiconductor Research Corporation for their contributions and funding allowing my research to thrive. It seems quite extraordinary in hindsight that what started out as an annual review meet for the SRC eventually led to me finding a job and embarking on a brand new adventure in my life.

Lastly, I would like to thank my parents; they have been a constant pillar of support for me be it for my move to half way across the planet or the struggles of daily life. They have always been there for me and I am deeply indebted to then for that.

Chapter 2, in part, has been submitted for publication of the material as it may appear in Applied Surface Science, 2019, Jong Youn Choi; Christopher F Ahles; Yunil Cho; Ashay Anurag; Keith T Wong; Srinivas D Nemani; Ellie Yieh and Andrew Kummel. "Selective Pulsed Chemical Vapor Deposition of Water-free HfOx on Si in Preference to SiCOH and Passivated SiO2." The author of this thesis was a co-author of this paper.

Abstract of the Thesis

Passivation for Selective ALD and CVD of Metals, Metal Oxides, and Metal Silicides

by

Ashay Anurag

Master of Science in NanoEngineering

University of California San Diego, 2019

Professor Andrew C. Kummel, Chair

As the scaling of nanoelectronic features continues well below the 5 nm node, conventional patterning mechanism like lithography and etching are unable to create aligned features with low margin errors and low line edge roughness. Atomic layer deposition (ALD) and chemical vapor deposition (CVD) help overcome this challenge. However, ALD typically leads to conformal deposition over the entire surface, without any control on the lateral arrangement of the atoms. Self-assembled monolayers (SAMs) can be used to locally deactivate the ALD growth if they can be selectively deposited. A critical issue with SAMS is that they are typically applied by using wet chemistry and are composed of long chain molecules (1-2nm) which require long deposition times to get molecular alignment which is needed for effective passivation.

This work reports effective vapor phase passivants for the application of self-assembled monolayers of small molecules to deactivate the selected ALD growth area. The passivants used are smaller than 1nm in length, create a film with RMS roughness of less than 5 Angstrom, and require low processing temperatures. Using one such passivant, [tetramethyldisilazane (TMDS)], up to 12nm of HfO_2 was deposited on Si without any deposition on passivated SiCOH and SiO_2. Deposition of metals including cobalt was also investigated by ALD. Contact angle was used to characterize the hydrophobicity of the surface; the surface topology was examined by atomic force microscopy (AFM), and the metal/metal oxide growth was characterized by x-ray photoelectron spectroscopy (XPS).

Chapter 1- Introduction

1.1 Selective deposition

Atomic layer deposition (ALD) processes exist for metals and metal oxides which obtain excellent conformality on high aspect ratio structures, but there is still a need for ALD processes which with high chemically selectivity. Ideal processes would include ones which nucleate well only on silicide or metal surfaces; this is challenging since surface defects on SiO_2 (Fig. (c) and (d)) and low-k dielectrics can cause unwanted nucleation[2]. Passivating the surface of SiO_2 can enhance the selectivity of ALD of metals, metal oxides and metal silicides by reducing unwanted nucleation as shown in Fig 1. In this work, the effectiveness of short chain organic monolayers, a passivation agent to enhance selective ALD, is investigated in contrast to longer chain self-assembled monolayers (SAMs).

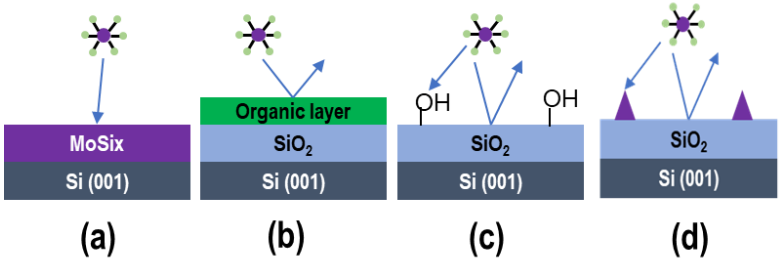

Figure 1. Schematic for selective passivation. (a) Interaction of precursor with the Si surface to deposit molybdenum silicide on Si[3]. (b) Organic layer preventing the interaction of precursor with surface. (c) Hydroxyl sites acting as active sites for precursor chemisorption. (d) Nucleation sites formed on the unpassivated surface.

To enhance the selectivity of ALD and CVD processes, SAMs composed of hexamethyl-disilazane[4] (HMDS) and octadecyl-trichlorosilane[5] (ODTS) have been used to block hydroxyl sites, preventing deposition of HfO_2 on SiO_2 without blocking deposition on Si or metals[6]. However, these SAMs have long alkyl chains -- they are not suitable for high aspect ratio vias and/or require liquid processing that take 24-48 hours for full effectiveness [7-9]. This work demonstrates the use of short

chain organic monolayers such as 1,1,3,3 tetramethyldisilazane (TMDS) and bis(N,Ndimethylamino)dimethylsilane[6] (DMADMS) as rapid acting vapor phase passivants, reducing the process time to a few seconds.

1.2 Atomic Layer Deposition and Chemical Vapor Deposition Fundamentals

Atomic layer deposition (ALD) is a vapor phase technique capable of producing thin conformal films of a variety of materials[2, 10]. A general ALD process consists of sequential alternating pulses of gaseous chemical precursors that react with the substrate through self-limiting processes and leave no more than one monolayer on the surface. After each pulse, the chamber is purged with an inert carrier gas (typically N_2 or Ar) to remove any unreacted precursor or reaction by-products. Due to its sequential and self-limiting nature, ALD produces features with conformality on high aspect ratio structures, thickness control at the angstrom level, and tunable film thickness and composition as shown in Fig 2. These processes are conducted at modest temperatures (25C to 300C), and the temperature range over which the growth rate per cycle is constant referred to as the 'ALD temperature window'. ALD is used to deposit a variety of materials, such as inert metals, metal oxides, nitrides, silicides etc.

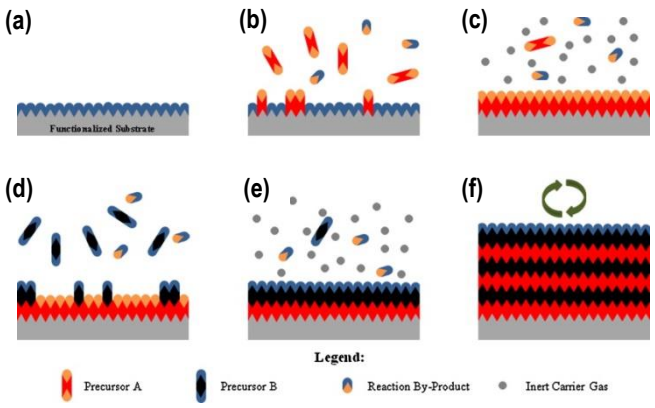

Figure 2. Typical steps in an ALD Process[2]. (a) The substrate surface has natural functionalization or is treated to functionalize the surface. (b) Precursor A is pulsed and reacts with surface. (c) Excess precursor and reaction by-products are purged with inert carrier gas. (d) Precursor B is pulsed and reacts with surface. (e) Excess precursor and reaction by-products are purged with inert carrier gas. Steps b–e are repeated until the desired material thickness is achieved in (f).

In this thesis, ALD was used to grow cobalt metal selectively on copper while inhibiting its growth on passivated SiO_2. Bis(1,4-di-tertbutyl-1,3-diazadienyl) cobalt [$Co(dad)_2$][11] and tert-butylamine [TBA]) were used for the ALD of cobalt.

Unlike ALD, chemical vapor deposition (CVD) is performed usually at elevated temperatures (200C to 900C); the high temperature induces the volatile precursors to decompose on the substrate surface[12]. CVD typically has a higher grown rate than ALD and sequential dosing of precursors is not employed. The reactions are not self-limiting and lack precise control over growth rate like ALD.

Pulsed CVD was employed for the deposition of hafnium oxide (HfO_x) using hafnium tert-butoxide (Hft(Bu)4). In pulsed CVD, a single precursor which spontaneous decomposes on reactive surfaces is employed. Pulsed CVD can provide conformal deposition on high aspect ratio structure when the sticking probability of the precursor is low. HfO_2 was selectively deposited on Si while little to no growth was observed on passivated SiO_2 and SiCOH.

1.3 Contact Angle

Contact angle is the angle made when a liquid drop (typically water) is place on a flat substrate. Water contact angles are used to characterize the hydrophobicity of the surface; a hydrophilic surface has contact angles between 0-20° while hydrophobic surfaces have angles closer to 90°. Highly hydrophobic surfaces can have contact angles greater than 90°.

Contact angles (herein meaning water contact angles) were used to measure the degree of hydrophobicity of the passivated surface. Contact angles were measured for HF cleaned SiO_2 and found to be less than 10°, after passivation the contact angles were observed to be around 90°.

1.4 Atomic Force Microscopy

Atomic Force Microscopy (AFM) was used to characterize the topology of the substrates. AFM is a scanning probe technique with a high resolution of surface features (typically ~1nm or less depending on the quality of the tip).

During contact mode AFM, the tip is brought into contact with the sample and scanned along the x and y directions. A feedback loop, which utilizes the cantilever deflection as input, is employed to keep the probe-sample force constant during scanning. Ultimately, changes in height are measured by a photodiode recording the change in the deflection of the cantilever as seen in Fig 3 [13]. AFM has the advantage in that it is simple and efficient at studying the roughness of ALD films when compared to other imaging technologies, such as SEM, TEM, or STM that have to use electron beam irradiation and/or high vacuum.

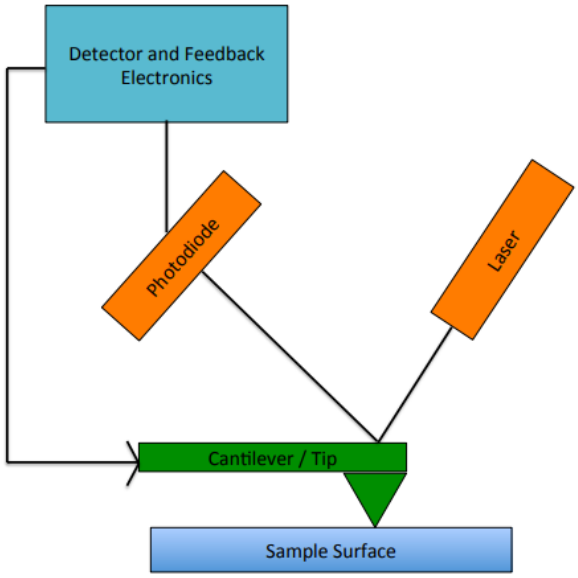

Figure 3. Details of AFM Operation. For contact mode, a tip is scanned across the sample surface and the changes in height are recorded through the deflection of the cantilever. Feedback from the detector and electronics keep the tip in contact with the surface.

1.5 X-Ray Photoelectron Spectroscopy

XPS was the characterization technique used to study the chemical composition of the various surfaces. Furthermore, the attenuation of the substrate peak was also used to estimate the thickness for the material deposited up to 5nm.

For XPS characterization, the substrate is exposed to a monochromatic x-ray; for this study, Al-coated anode is used with the incoming energy Al Kα radiation of 1486.7 eV, and a series of lenses confine the spot size to 1.2 mm. The x-rays excite the core and valence electrons of the surface atoms and ejects them with a discrete characteristic kinetic energy. A hemispherical multichannel analyzer collects the electrons, along with a set electron pass energy that applies voltages to retard or accelerate the collected electrons. To amplify the signal from the collected electrons, a 5-channel electron multiplier is used to amplify current[14]. The electron count, adjusted for the sensitivity, provides the relative percentage of the corresponding atoms and their chemical state. The kinetic energies (KE) of the electrons are measured by the detector, and binding energy (BE) are calculated by subtracting the KE from for the incoming energy of the x-rays along with the difference in work function of the spectrometer (Φspec) and substrate [15]. It is possible to perform broad survey scans as well as high resolution narrow scans with spectral resolution up to 0.1ev.

In this work, XPS is employed to characterize the chemical composition on the surface of the substrate. The normalized XPS peak can also be used to estimate the thickness of the film based on the attenuation of the substrate.

Chapter 2- Passivation for Selective ALD and CVD of Metals, Metal Oxides, and Metal Silicides

2.1 Background

Self-assembled monolayers (SAM) are organic molecules that spontaneously adsorb onto various materials, typically onto the surface of solid substrates. SAM monomers consists of a headgroup which binds to the surface, an alkyl chain that ensures the ordering in a monolayer, and a tail group that determines the character of the surface after functionalization[12]. SAMs can bind to the surface by means of chemisorption and physisorption, and have applications across many fields like pharmaceuticals, sensors and microprocessors [16-18]. This study focuses on the application of SAMs for semiconductor fabrication. Generally, SAMs are exposed to the substrate in appropriate conditions to chemisorb (i.e. covalent bond) to the substrate. Once adsorbed, the tail group determines the character of the substrate. For instance, using SAMs with CH_3 or CF_3 tail groups, the surface becomes unreactive toward most ALDs because the C-H and C-F bonds are stable and the polarizability is low, so precursor physisorption is decreased.

Since the early 1990s, long chained alkylsilanes like octadecyl-trichlorosilane (ODTS)[5, 19] have been extensively studied and found to form well-ordered, closely packed monolayers with great thermal stability on hydroxyl terminated SiO_2. Substrates passivated with ODTS have contact angles of about 100° with RMS roughness of 0.8 nm[19]. ODTS passivation requires 24 hours by liquid phase in 24 hours and 30 minutes by vapor phase reaction. However, with decreasing critical dimension sizes in semiconductor vias, using the 2.6nm [20] large molecule is not feasible.

An alternative to using long chain alkylsilanes is to use short chain functionalized SAMs like aminopropyltriethoxysilanes (APTES)[7, 21] and mercaptopropyltrimethoxysilanes (MPTMS)[8]. These molecules are smaller than a nanometer in length and produce modest contact angles of 75-80°; APTES,

however, has low thermal stability (200°C) and MPTMS produces quite rough surfaces as it often undergoes self-polymerization. Moreover, both the passivants require liquid phase processing for up to 2 hours to get effective coverage.

The most commonly uses passivant in the industry currently is 1,1,1,3,3,3-hexamethyl-disilazane (HMDS)[4]. HMDS is primarily used as an adhesion layer between the substrate and photoresist for lithography[22]. These molecules are smaller than 1 nm and form smooth monolayers on the substrate. HMDS has been reported to enhance the selectivity in hafnium oxide deposition, even more than ODTS[4]. These molecules can passivate substrates in the liquid as well as vapor phases. However, liquid phase HMDS passivation requires temperatures as high as 110°C for 24 hours and vapor phase passivation requires the temperature as high as 280°C[4]. Besides high processing temperatures and times, these passivants have been reported to have low coverage leaving several exposed sites vulnerable to ALD[19].

Despite having several SAMs available, there is a large scope for improvement in the size, coverage, processing temperature and phase of the passivants to meet the industry standards. This study explores the viability of two passivants namely 1,1,3,3-tetramethyldisilazane (TMDS) and bis(dimethylamino)dimethylsilane (DMAMDS). Fig 4 displays the structure of these molecules. Both passivants react by breaking the Si-N and SI-H bonds, and it is assumed that the Si-CH_3 bonds are stable in both molecules. TMDS is similar to HMDS with 2 methyl groups per silicon instead of 3, and it is expected that the lack of methyl groups would decrease the steric interaction, enabling better coverage. DMADMS has been reported to enable selective ALD of ruthenium metal on SiO_2[6] , and it has been studied for its ability to inhibit ALD on oxides[22].

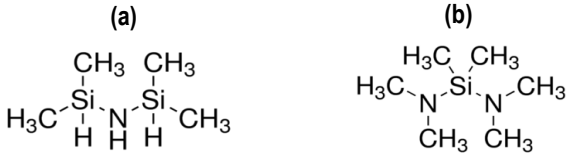

Figure 4. Structure of passivants (a) TMDS and (b) DMADMS molecules.

2.2 Experiment

1,1,3,3-tetramethyldisilazane (TMDS) (97%, Sigma Aldrich), bis(dimethylamino)dimethylsilane (DMAMDS) (>95%, Sigma Aldrich) and N1-(3-trimethoxysilylpropyl)diethylenetriamine (DETA) (>85%, Sigma Millipore) were used as passivation agents on SiO_2 and SiCOH. SiO_2 was loaded for passivation after degreasing the surface using acetone, methanol and HPLC grade water for 30 seconds each, followed by a 30 second dip in a 0.5% HF(aq) solution. The SiCOH surface was degreased using the same process but without the HF clean.

2.2.1 Liquid Phase Passivation

All liquid phase reactions were performed in a nitrogen glove box. Substrates were passivated by a solution of TMDS and toluene (99+%, Fischer Scientific) which was optimized to 1% by volume. SiO_2 was dipped in 2ml of the solution for 24 hours at 70°C. After passivation, hexane was used to remove residual TMDS particles by sonication. The substrates were dried with a nitrogen gun and were subsequently measured for its contact angle and surface topology.

2.2.2 Vapor Phase Passivation

The vapor phase passivation was done in a separate chamber where the base pressure was 200 mtorr pumped by a mechanical pump (Edwards RV3). The chamber was consisted of a sample stage which had a cartridge heater to raise the sample temperature. Fig 5 shows a schematic diagram of the chamber with the passivant inlets and the nitrogen line. The walls were wrapped with heat tape for hot wall conditions.

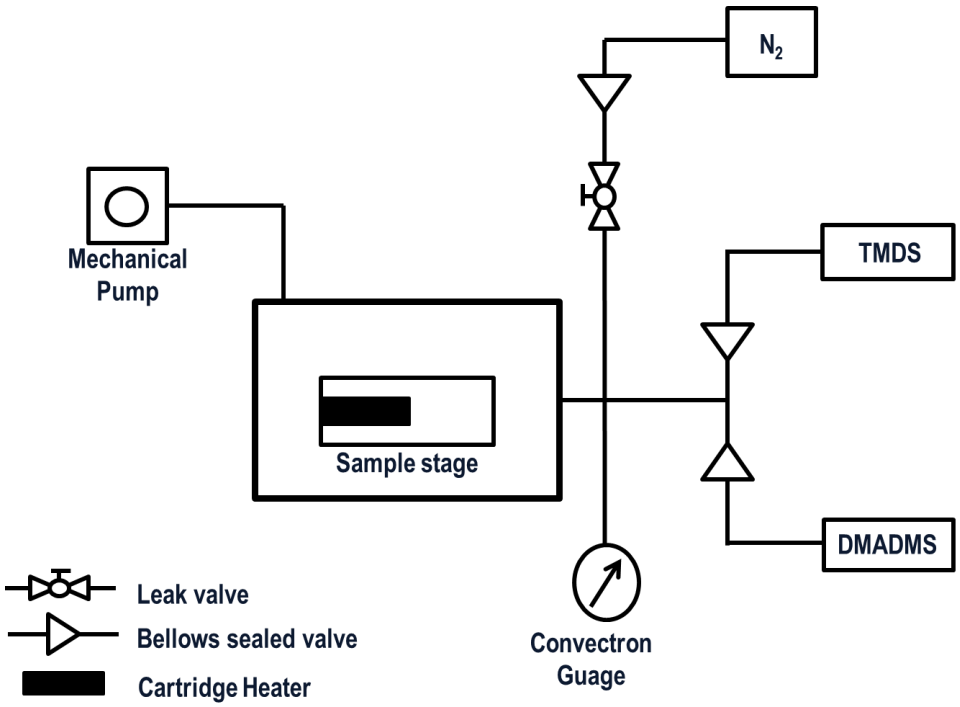

Figure 5. Schematic of vacuum passivation chamber. The chamber was composed of a heated stage, two inlet lines for passivants and a N_2 purge line.

The chamber wall was kept at room temperature and the precursor bottles were kept at room temperature for TMDS and DMADMS. The passivants continuously flowed into the chamber for an optimized time for each passivant using a bellows sealed valve. The optimized reaction temperature was determined to be 70°C for TMDS and DMADMS.

After the passivation process, the passivated SiO_2 and passivated SiCOH were quickly loaded into a separate sample loading chamber that was connected to the reaction chamber and UHV chamber to minimize the contamination from the air transfer and perform the subsequent ALD and CVD reactions.

2.3 Results and discussion

Following the passivation, the hydrophobicity of the substrates was measured by contact angle, and its topology was studied by AFM. The passivated samples were also tested for selectivity after deposition by performing XPS. The results for each passivant are discussed in detail for each passivant.

2.3.1 Liquid phase

Liquid phase passivation of SiO_2 substrate increased contact angle and produced smooth films. Fig. 6(a) shows a degreased SiO_2 substrate with a contact angle of 50°. Upon passivation, its contact angle increases to 90°, indicating increased hydrophobicity for both 2 hr (Fig. 6(b) and 24 hr (Fig. 6(c)) passivation. The roughness of all 3 substrates was observed to be about 2-3Å. In general, when multiple samples are run, the contact angles are reproducible to 85° and standard errors of about 82° for sample made in triplicate; therefore, any changes in contact angle of 85° are significant. A more detailed example is shown below.

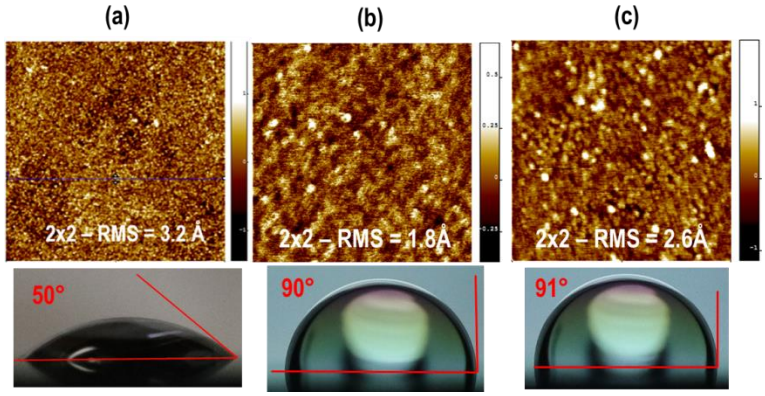

Figure 6. Representative AFM and contact angle: (a) Unpassivated SiO_2, (b) 2hr liquid passivated TMDS on SiO_2, (c) 24hr liquid passivated TMDS on SiO_2 at 70°C.

To test the passivants' thermal stability, multiple substrates were annealed at 350°C for 30 min at 5 x 10^{-5} torr. Fig. 7 shows the average water contact angles before and after annealing for five different

substrates after different passivation conditions. The data in Fig.7 shows the 24 hr passivated sample had a statistically similar contact angle before and after annealing; this was also the same contact angle as found on the 2 hr passivated sample before annealing. The decrease in the contact angle upon annealing for the 2 hr passivated sample suggests that 2 hours is not sufficient time to form robust Si-O bonds[23]; therefore, upon annealing, some of the TMDS molecules desorb, reducing the hydrophobicity.

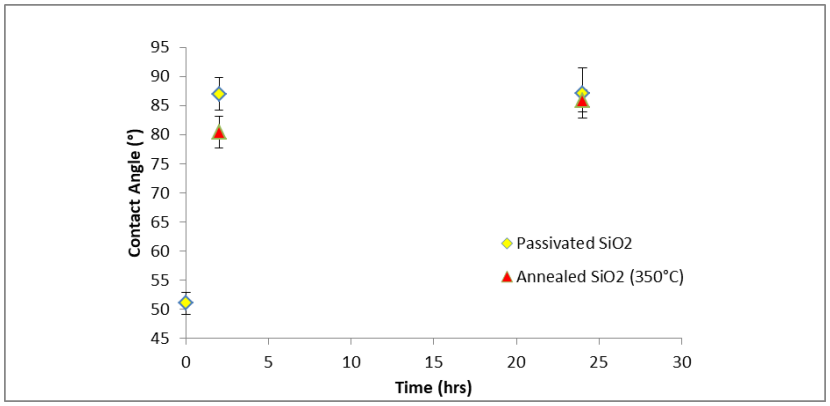

Figure 7. Contact angle after liquid passivation before vs after anneal. Gold data points show sample passivation at 70 °C for 0 hr, 2 hr, and 24 hrs. Red data points show the effect of subsequent annealing at 350 °C for 30 min at $5x10^{-5}$ torr. For the 2 hr passivated sample, the contact angle decreases after annealing. The error bars are standard deviations.

XPS was performed on the 24 hr passivated substrate (Fig 8). Upon UHV anneal, most of the physisorbed carbon is removed; however, there is almost 3 times more carbon content on the passivated substrate as compared to the unpassivated substrates consistent with the carbon from passivating methyl groups in TMDS being chemisorbed to the substrate. Note the nitrogen content is <2% before and after anneal on the passivated sample consistent with desorption of nitrogen during the liquid passivation process.

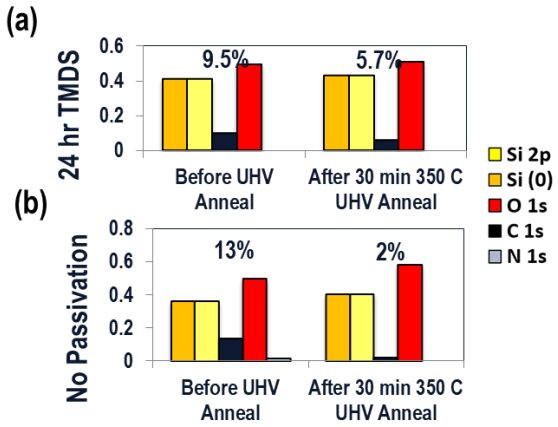

Figure 8. XPS peaks obtained before and after UHV anneal for 30 min: (a) 24 hr liq. passivated SiO_2 at 70°C and (b) Unpassivated SiO_2. UHV anneal reduces C.

The hydrophobicity of TMDS was compared with that of 1,1,1,3,3,3-hexamethyldisilazane (HMDS). Fig.9 (a) and (b) compare the contact angle under same liquid passivation conditions. For 24 hr liquid passivation at 70°C, TMDS provided a contact angle of 91° whereas contact angle for HMDS was 73°. Fig.9 (c) is the contact angle obtained upon liquid passivation of HMDS at 110°C which provided a contact angle of 74°. The passivation was also done at 110°C, which was the best process condition reported in literature[4]. The contact angle is higher for TMDS as compared to HMDS in all cases. Since HMDS has 3 methyl groups on each Si atom, it is expected to produce very hydrophobic surface for complete monolayer coverage. It is likely that the low contact angle is a consequence of lower coverage on the substrate, which is likely caused by high steric hindrance due to three methyl groups as shown in Fig. 10. In case of TMDS, while each monomer might not be as hydrophobic as HMDS due to the presence on only 2 methyl groups (Fig. 4(a)); the lower steric hindrance may facilitate efficient packing making the surface overall more hydrophobic.

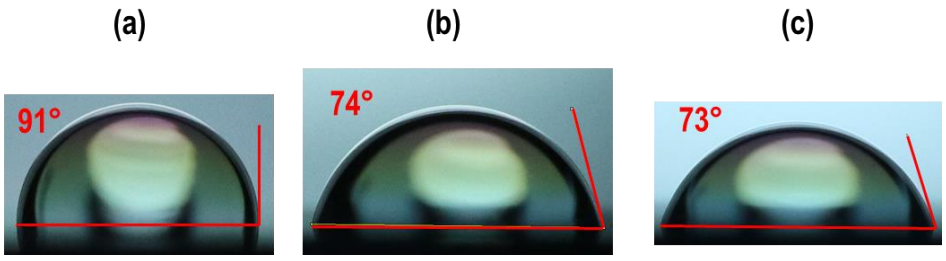

Figure 9. Contact angles after 24 hr liquid passivation: (a) TMDS at 70°C (b) HMDS at 70°C and (c) HMDS at 110°C.

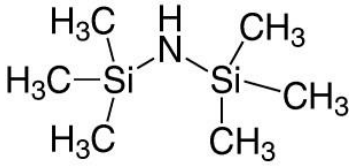

Figure 10. Structure of HMDS. Each Si atom has 3 methyl groups.

The efficacy of the liquid passivant was tested for the deposition of molybdenum silicide ($MoSi_X$). $MoSi_x$ deposited by 50 ms MoF_6 and 18 ms Si_2H_6 doses and pump time of 2 min between doses at 120°C has an inherent selectivity to silicon and does not deposit on SiO_2[3]. However, the unpassivated hydroxyl sites on SiO_2 often act as nucleation sites leading to unwanted deposition. Fig. 11 shows the XPS and AFM of the deposition on Si, unpassivated SiO_2 and passivated SiO_2. After 5 ALD cycles, the normalized molybdenum peak is a factor of 5 lower on the passivated and unpassivated SiO_2. The data is consistent with $MoSi_x$ ALD being inhibited even on unpassivated SiO_2 and shows liquid TMDS passivation further decrease the reactivity of the SiO_2. AFM was obtained to study the surface morphology which shows the number of nucleation sites is reduced from by a factor of 7, from 285 nuclei/μm^2 to 40 nuclei/ μm^2 consistent with the TMDS passivating most of the hydroxyl sites.

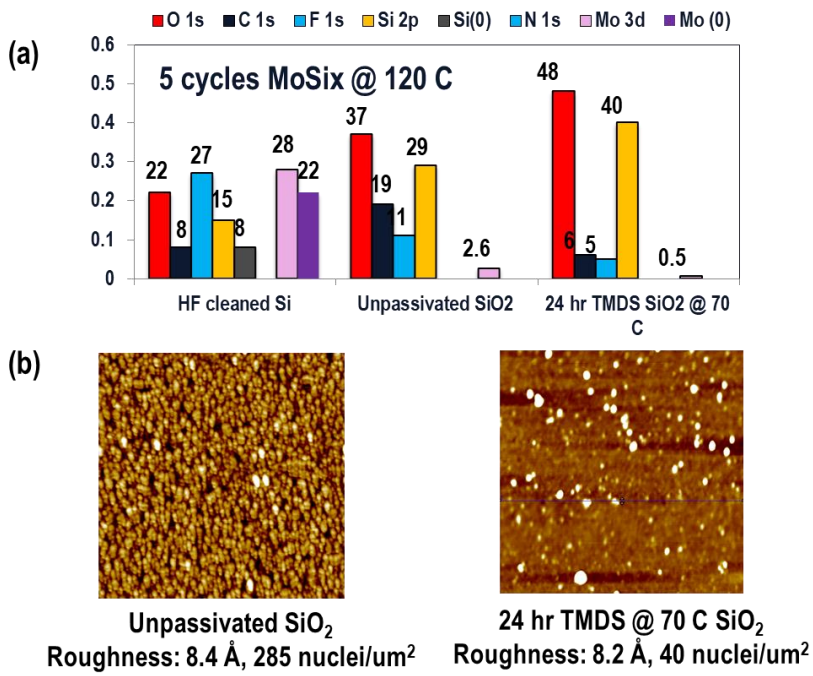

Figure 11. Selective $MoSi_x$ ALD on unpassivated and liquid TMDS passivated SiO_2. (a) XPS signals obtained from three substrates, namely, Si (growth substrate), unpassivated SiO_2 (non-growth substrate) and SiO_2 passivated with 1% (by vol.) TMDS solution in toluene at 70°C in N_2 environment, (non-growth substrate). (b) Representative AFM of the passivated and unpassivated SiO_2 after $MoSi_x$ ALD with calculated nucleation densities. The ALD was performed with 50 ms MoF_6 dose and 18 ms Si_2H_6 dose at 120°C, the pump time between doses was 2 min. TMDS passivation reduced the density of unwanted nuclei by 7x.

2.3.2 Vapor Phase

As shown in Fig. 12 (a) &(b), 10 min exposure of vapor phase TDMS at 70 ^{o}C and 7 Torr or a 10 second exposure of DMADMS at 70 ^{o}C and 5.5 torr are sufficient to nearly match the contact angle of liquid phase TDMS shown in Fig 6(b). As shown in the AFM images, the vapor passivation creates a smooth surface with roughness of about 2 Å. It was hypothesized that the vapor passivation might not be complete; therefore, samples were exposed to a second vapor passivation cycle. Fig.12 (c) & (d) shows the contact angle upon double passivation, in two different orders. While the contact angle does not change significantly upon dosing DMADMS on the sample previously passivated with TMDS, the

contact angle changes significantly upon dosing TMDS on the sample previously passivated with DMADMS, increasing from 82° to 91°.

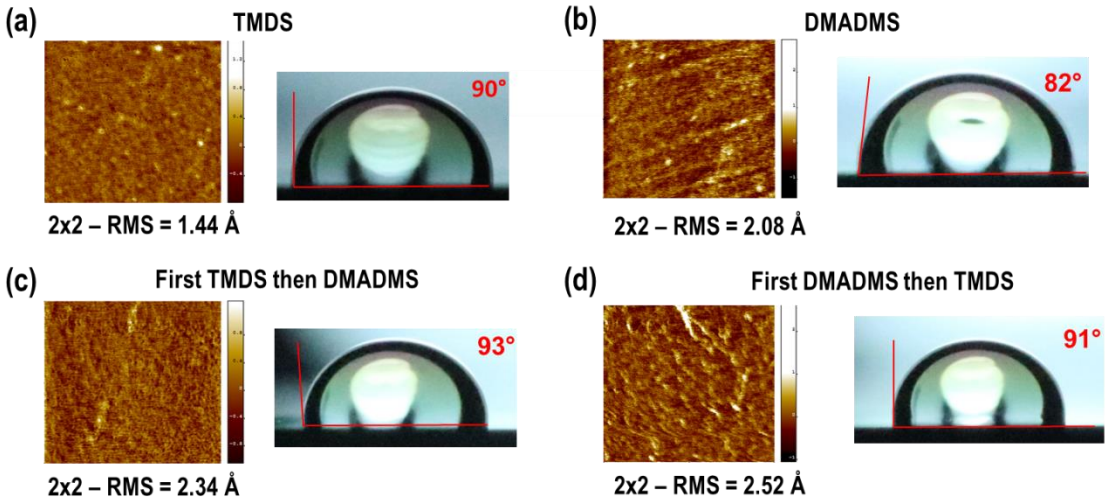

Figure 12. Representative AFM topology and contact angle of passivated SiO_2 substrate with: (a) TMDS passivated at 70 °C for 10 min at 7torr, (b) DMADMS passivated at 70 °C for 10 sec at 5.5 torr, (c) first TMDS then DMADMS passivated at 70 °C for a total of 11 min, pressure was 7 torr for TMDS and 5.5 torr for DMADMS and (d) first DMADMS then TMDS passivated at 70 °C for a total of 11 min, pressure was 5.5 torr for DMADMS and 7 torr for TMDS.

It is hypothesized that the contact angle by DMADMS is slightly smaller due to its bulkiness as compared to TMDS which may create less dense packing. Fig. 13 illustrates the proposed mechanism for the passivation of each molecule. The DMADMS molecule comprises of only one Si atom and 2 bulky nitrogen groups. It is likely that due to this bulkiness, the packing is sparse and not all the OH sites are bonded with the silicon. Additionally, DMADMS can bond dually as well as form a monodentate bonds (Fig. 13) with no appreciable difference in energy[6]. In case of TMDS, although similar in size compared to DMADMS, since one molecule of TMDS contains 2 silicon atoms, it is hypothesized that increases the coverage. However, since TMDS cannot form monodentate bonds, it is likely there will be sparsely scattered single OH defect sites on the TMDS passivated surface.

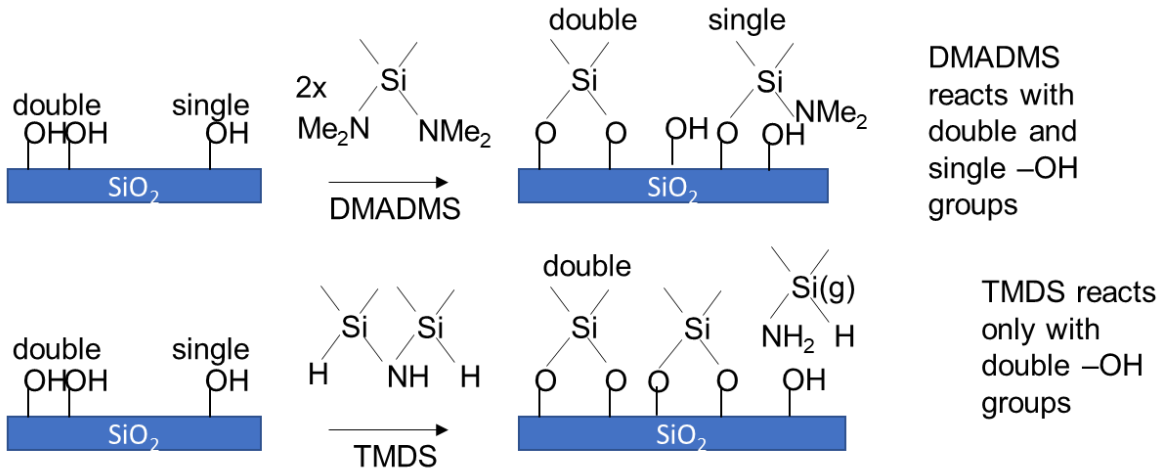

Figure 13. Proposed passivation mechanisms for TMDS and DMADMS on SiO_2 substrate.

Since it is already known that DMADMS can passivate SiO_2 for selective Ru ALD[6], the passivation was tested for oxide ALD since this is more challenging. XPS was used to evaluate the efficacy of the gas phase passivation by TDMS and DMADMS using HfO_2 pulsed CVD since $Hf(O^tBu)_4$ readily reacts with SiO_2 but is less reactive towards SiCOH (which is a CH_3 terminated porous SiO_2). On unpassivated SiO_2, deposition proceeds readily and an amorphous HfO_2 film is deposited as evidenced by the 18% Hf and attenuation of the Si 2p peak in Fig 14. The gas phase TMDS passivated SiO_2 inhibited the HfO_2 deposition compared to a bare SiO_2 substrate but shows less selectivity for the CVD process than SiCOH. As seen in Fig. 14, based on the attenuation of the substrate peak, after 11 cycles of pulsed $Hf(O^tBu)_4$ at 250°C, 0.84 nm of HfO_2 is deposited on unpassivated SiO_2 while only 0.24 nm is deposited on the passivated SiO_2, SiCOH shows the least amount of deposition, 0.13nm.

Furthermore, gas phase DMADMS passivation on SiO_2 had less selectivity than gas phase TMDS passivated SiO_2 as shown in Fig 15. The data is consistent with the bulkier DMADMS reducing surface packing density despite the DMADMS only requiring only one active site. This is consistent with the

defects due to loose packing being more detrimental to oxide selective deposition than the isolated reactive sites in the TMDS passivation.

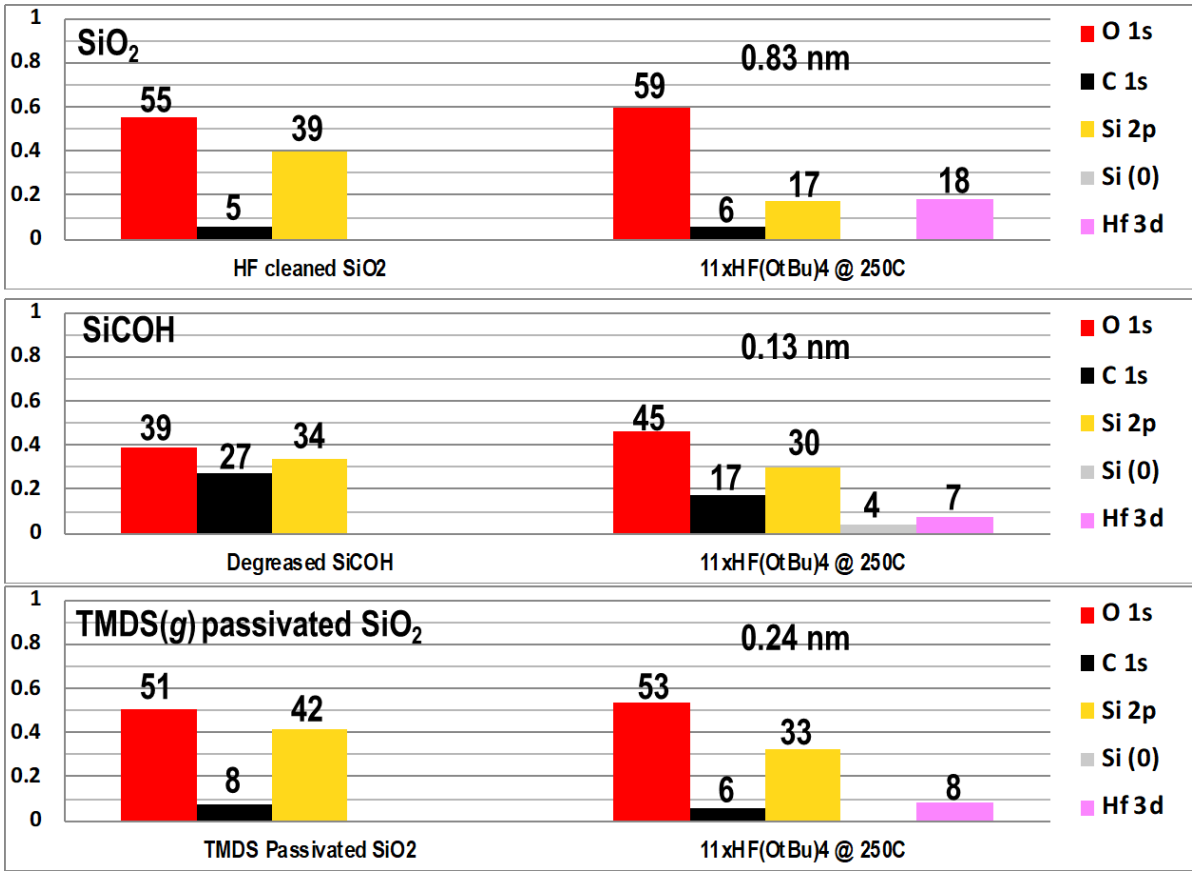

Figure 14. XPS of HfO_2 CVD on SiO_2 and SiCOH: Normalized concentrations showing reduction in Hf deposited by 11 cycles of (2-3mTorr) $Hf(O^tBu)_4$ doses at 250 °C with 60 s purge and cont. N_2 purge(130mTorr) on unpassivated SiO_2, SiCOH and SiO_2 passivated with vapor phase TMDS passivated at 70 °C for 10 min at 7 torr.

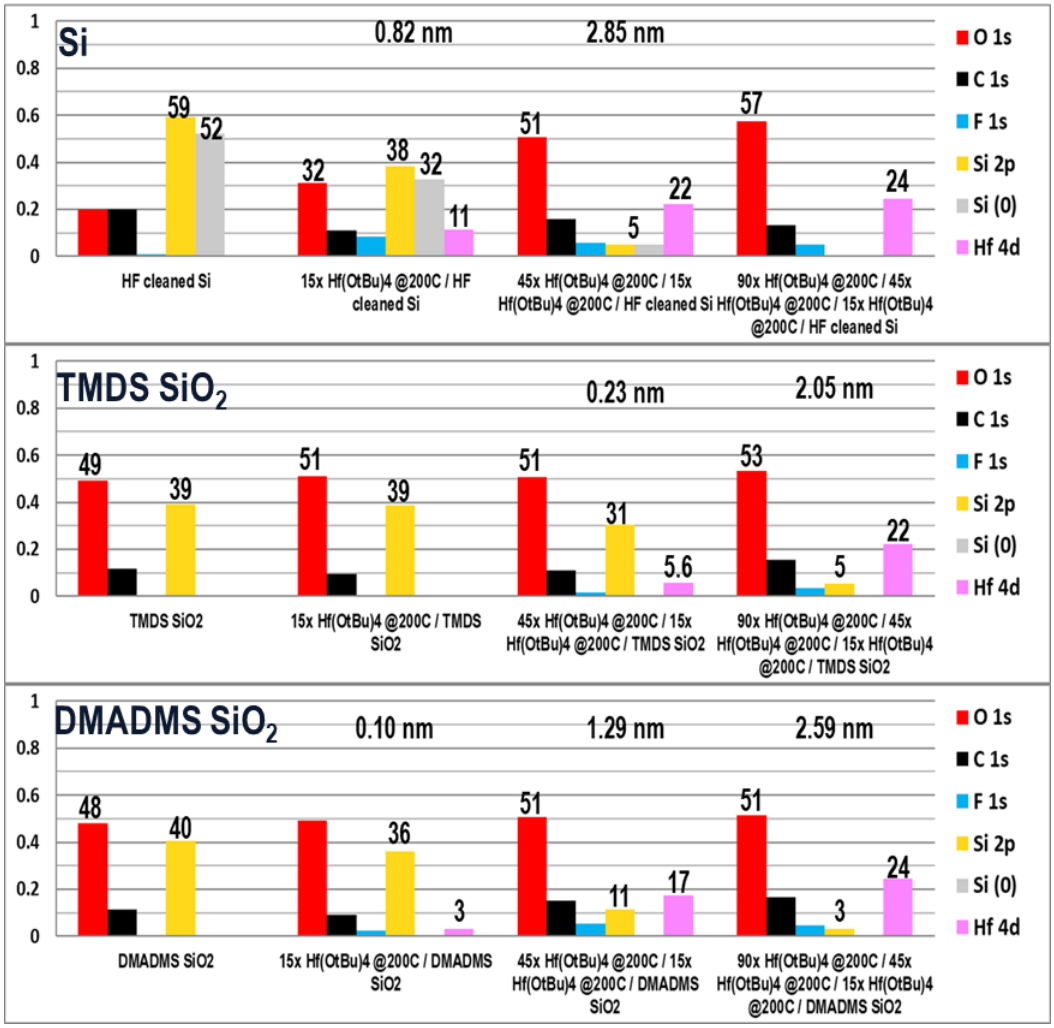

Figure 15. XPS of HfO_2 CVD on Si and passivated SiO_2: Normalized concentrations showing reduction in Hf deposited by $Hf(O^tBu)_4$ doses at 200 °C with 50ms (3mTorr) pulses, 15 sec wait, and continuous N_2 purge (130 mTorr) on SiO_2 passivated with vapor phase TMDS at 70 °C for 10 min at 7 torr and DMADMS passivated at 70 °C for 10 sec at 5.5 torr.

Two models may explain TMDS being a better gas phase passivant than DMADMS: either TMDS sticks better to the surface i.e. it creates less defects or TMDS makes the surface more hydrophobic i.e. the hafnium butoxide precursor has lower sticking on TMDS compared to a DMADMS passivated surface. More experiments on the effect of purge time are needed to determine which hypothesis is correct.

In Fig. 16, the selectivity of different combinations of passivants and substrates were compared as a function of HfO_2 thickness on Si. $S = T_G/T_{NG}$ was used as a metric of the selectivity, where T_G is HfO_x thickness on the growth area and T_{NG} is HfO_x thickness on the non-growth area. The growth area was Si and the non-growth areas were SiCOH, passivated SiO_2 and passivated SiCOH. The HfO_x thicknesses were calculated using the XPS attenuation method and ellipsometry. A control sample of OH-terminated SiO_2 showed the same growth rate of HfO_2 as on Si; therefore the selectivity metric was close to unity: S = 1.05. The TMDS passivated SiO_2 showed high selectivity at (S=12.4) for T_G = 2.85 nm; the selectivity decreased to S=5.32 for T_G = 10.68 nm. This is consistent with the general model of selectivity loss: after a large number of precursor dosing cycles, sufficient precursor gets adsorbed on the passivated surface and this layer of reactive nuclei templates oxide growth. This mechanism results in a delay in growth on the passivated surfaces consistent with TMDS passivating -OH groups on SiO_2. DMADMS did not perform as well as TMDS; this is likely due to the poor coverage of DMADMS consistent with the data in Fig 12.

The combinations of TMDS and DMAMDS were tested to passivate SiO_2. (D+T) denotes a sequential passivation of DMADMS followed by TMDS, (T+D) is the opposite order of the passivants. (D+T) SiO_2 showed S=7.91 at T_G=2.85 and S= and 3.43 at T_G=8.5 nm which is similar to TMDS alone. (T+D) SiO_2 exhibited similar or slightly lower selectivity than DMADMS-SiO_2. For SiO_2, the passivation using two passivants were not as effective as using a single passivants and the order of the passivants matters. The importance of the order is likely due to the properties of the terminal passivant. Since it is hypothesized that the coverage by DMADMS is insufficient, exposure to TMDS increases the hydrophobicity as is seen by the change in contact angle (Fig. 12 (b) and (d)) which in turn is likely to enhance the selectivity. As is seen in Fig 16, DMADMS first then TMDS (D+T) SiCOH showed the best selectivity of S = 16.76 at T_G = 2.85 nm. This corresponds to and 0.17 nm thick HfO_x on (D+T) SiCOH and xxx on SiO_2. Compared to the degreased SiCOH (S=3.45 at T_G=2.38), the selectivity increased by a

factor of ~5 by employing TMDS and DMADMS passivants. This is consistent with the reactive -OH sites on SiCOH can be effectively passivated by the passivants.

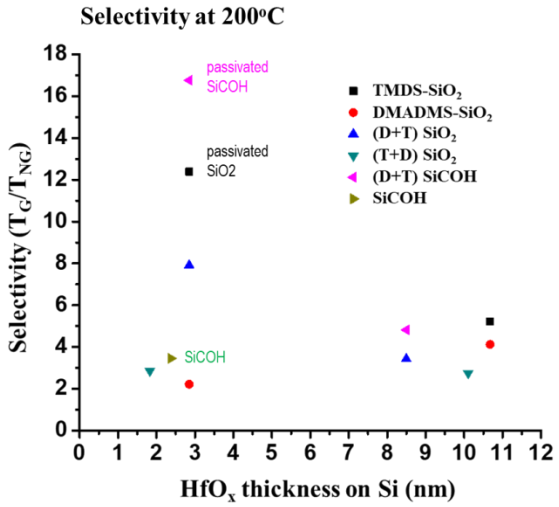

Figure 16. Selectivity metric (S) of passivated SiO_2 and SiCOH as a function of HfO_x thickness on Si. TMDS was the most effective passivant on OH-terminated SiO_2. The HfO_x was deposited by $Hf(O^tBu)_4$ doses at 200 °C with 50ms (3mTorr) pulses, 15 sec wait, and continuous N_2 purge (130 mTorr). SiO_2 and SiCOH were passivated with vapor phase TMDS at 70 °C for 10 min at 7 torr and passivated vapor phase DMADMS at 70 °C for 10sec at 5.5 torr .

2.4 Selective passivation for selective Co ALD on copper

Copper exposed to atmosphere was degreased as discussed in the experiment section and passivated with TMDS. Atmosphere exposed copper has a thin oxide layer on the surface; therefore, TMDS passivated the Cu. Fig. 17 (a) and (b) shows the change in contact angle from 50° to 80° after passivation, indicating an increase in the hydrophobicity. However, upon annealing, in ultra-high vacuum, the copper oxide desorbs along with the TMDS exposing a clean copper surface. This is illustrated in Fig. 17 (c) and (d) which shows the change in contact angle before and after anneal for an unpassivated and passivated Cu sample. After UHV anneal, the contact angle for the unpassivated sample shows little change, but the XPS spectra in Fig. 17(e) reveals a sharp decrease in the normalized carbon and oxygen peaks from 51% and 33% to 2.7% and 2.4% respectively while the Cu peak has increased from 12% to

94% indicated that the adventitious carbon and copper oxides have desorbed exposing the Cu metal. For the passivated sample, Fig. 17 (f) shows the disappearance of Si peak from the spectra indicating that TMDS is no longer present on the surface in addition to the liftoff shown in the unpassivated sample.

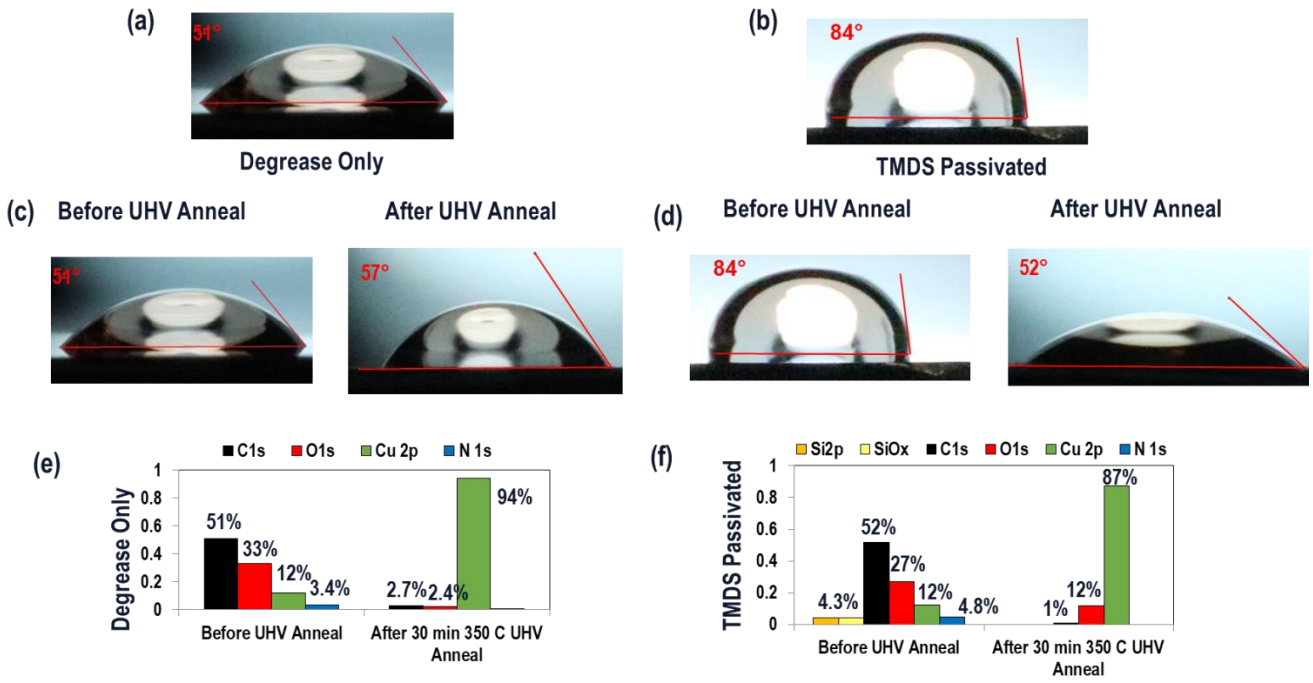

Figure 17. Properties of passivated and unpassivated copper: (a) Contact angle of a degreased Cu substrate, (b) Contact angle of passivated Cu substrate, (c) Contact angle of degreased Cu substrate before and after UHV anneal, (d) Contact angle of Passivated Cu substrate before and after UHV anneal, (e) XPS spectra of degreased Cu substrate before and after UHV anneal, (f) XPS spectra of Passivated Cu substrate before and after UHV anneal. Copper was passivated with 1% (by vol.) TMDS solution in toluene at 70°C in N_2 environment.

Desorption of TMDS is not observed from SiO_2 because the Si-O bonds do not break at modest temperatures. This difference can be used to selectively deposit films on copper without depositing film on SiO_2. Fig. 18 shows the SEM image of a cobalt ALD process on a Cu/SiO_2 tiger-stripe vapor TMDS passivated and unpassivated substrates. The dark regions in the tiger-stripe are the SiO_2. The unwanted ALD on the SiO_2 appear as small grey nuclei on the black regions. For the unpassivated sample, a large density of nuclei is observed. On the passivated substrate, the nuclei density is greatly reduced on the

SiO_2, indicating that the TMDS decreased the deposition of cobalt on the SiO_2 consistent with selective passivation.

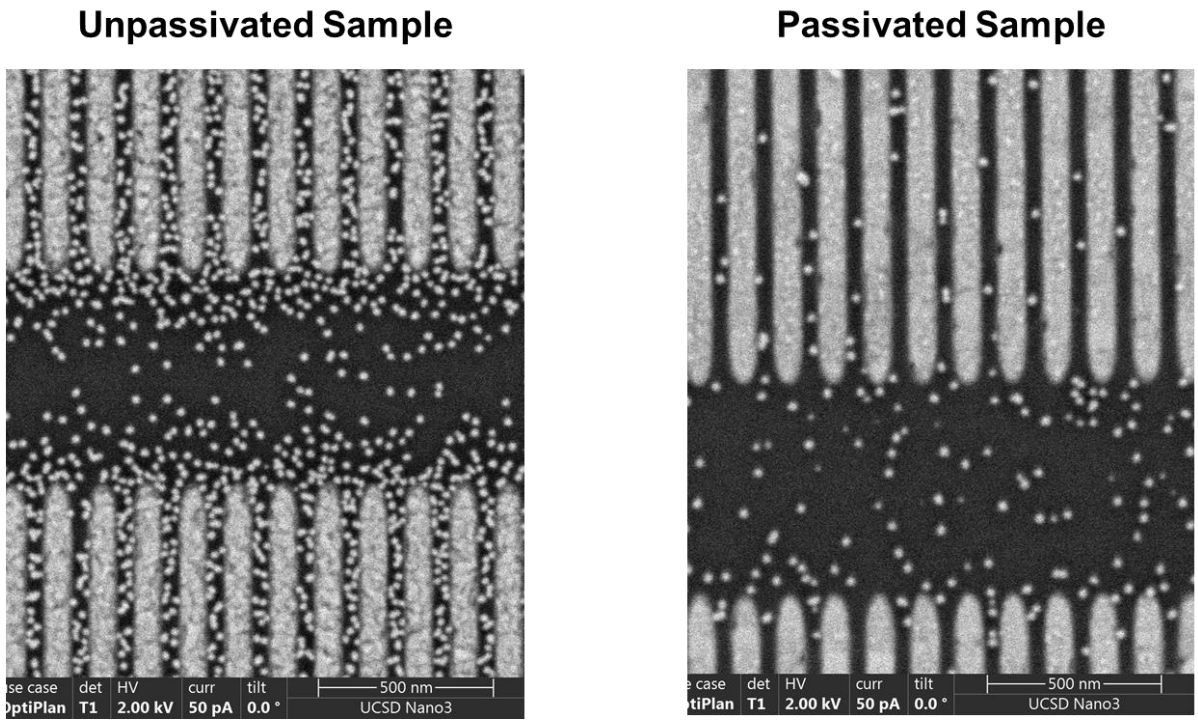

Figure 18. SEM image of cobalt ALD on unpassivated and passivated patterned samples. (a) Unpassivated patterned Cu (grey)/SiO_2 (black) samples. (b) Passivated patterned Cu (grey)/SiO_2 (black) samples (vapor phase TMDS at 70°C for 10min at 7torr) Co ALD employs 8 pulses bis(1,4-di-tert-butyl-1,3-diazadienyl) cobalt [Co(dad)2] at 200 mtorr per half cycle and 2 pulses of tert-butylamine (TBA) at 1 torr per half cycle at 180ºC.

TMDS shows passivation properties for both HfO_x and Co deposition despite no similarities in the precursors. The precursors will have different steric and hydrophilic properties yet TMDS shows resistance to both these passivants, which indicates that the TMDS is strongly bound to the surface and occupied most of the active sites, preventing the interaction of these precursors with the SiO_2.

2.5 Summary

This work demonstrates the effectiveness of rapid passivation of small sized passivants in the vapor phase at low temperatures. It can be hypothesized that DMADMS requires only 1 active site for passivation while TMDS requires 2 adjacent sites. Since DMADMS group are bulky, the packing is loose, thus having lower contact angle despite being more hydrophobic. This loose packing creates more defects compared to TMDS, consistent with TMDS having better passivation properties. It is unclear whether TMDS strongly binds to the surface and occupies most of the active sites preventing the interaction of these precursors or if the TMDS makes the surface sufficiently hydrophobic to prevent the precursors from interacting with the surface. Since the TMDS passivated substrate was not affected by different precursors, such as $Hf(O^tBu)_4$ and $Co(DAD)_2$ with no structural or chemical similarities, the data suggest that TMDS bonded strongly with the hydroxyl groups on the surface thus preventing precursor adsorption. On copper, it is observed that TMDS passivants copper but desorbs from copper after annealing enabling selective deposition on metal with decreased deposition on passivated SiO_2.

Chapter 2, in part, has been submitted for publication of the material as it may appear in Applied Surface Science, 2019, Jong Youn Choi; Christopher F Ahles; Yunil Cho; Ashay Anurag; Keith T Wong; Srinivas D Nemani; Ellie Yieh and Andrew Kummel. “Selective Pulsed Chemical Vapor Deposition of Water-free HfOx on Si in Preference to SiCOH and Passivated SiO2.” The author of this thesis was a co-author of this paper.

References

1. Mackus, A.J.M., M.J.M. Merkx, and W.M.M. Kessels, *From the Bottom-Up: Toward Area-Selective Atomic Layer Deposition with High Selectivity.* Chemistry of Materials, 2019. **31**(1): p. 2-12.

2. Johnson, R.W., A. Hultqvist, and S.F. Bent, *A brief review of atomic layer deposition: from fundamentals to applications.* Materials Today, 2014. **17**(5): p. 236-246.

3. Choi, J.Y., Ahles, C. F., Hung, R., Kim, N., Kummel, A. C., *Selective atomic layer deposition of MoSix on Si (0 0 1) in preference to silicon nitride and silicon oxide.* Applied Surface Science, 2018. **462**: p. 1008-1016.

4. Guo, L. and F. Zaera, *Spatial resolution in thin film deposition on silicon surfaces by combining silylation and UV/ozonolysis.* Nanotechnology, 2014. **25**(50): p. 504006.

5. Chen, R. and S.F. Bent, *Chemistry for Positive Pattern Transfer Using Area-Selective Atomic Layer Deposition.* Advanced Materials, 2006. **18**(8): p. 1086-1090.

6. Khan, R., Shong, B., Ko, B. G., Lee, J. K., Lee, H., Park, J. Y., Oh, I. K., Raya, S. S., Hong, H. M., Chung, K. B., Luber, E. J., Kim, Y. S., Lee, C. H., Kim, W. H., Lee, H. B. R., *Area-Selective Atomic Layer Deposition Using Si Precursors as Inhibitors.* Chemistry of Materials, 2018. **30**(21): p. 7603-7610.

7. Pasternack, R.M., S. Rivillon Amy, and Y.J. Chabal, *Attachment of 3-(Aminopropyl)triethoxysilane on Silicon Oxide Surfaces: Dependence on Solution Temperature.* Langmuir, 2008. **24**(22): p. 12963-12971.

8. Hu, M., Noda, S., Okubo, T., Yamaguchi, Y., Komiyama, H., *Structure and morphology of self-assembled 3-mercaptopropyltrimethoxysilane layers on silicon oxide.* Applied Surface Science, 2001. **181**(3): p. 307-316.

9. Maestre Caro, A., Maes, G., Borghs, G., Whelan, C. M., *Screening self-assembled monolayers as Cu diffusion barriers.* Microelectronic Engineering, 2008. **85**(10): p. 2047-2050.

10. George, S.M., *Atomic Layer Deposition: An Overview.* Chemical Reviews, 2010. **110**(1): p. 111-131.

11. Kerrigan, M.M., J.P. Klesko, and C.H. Winter, *Low Temperature, Selective Atomic Layer Deposition of Cobalt Metal Films Using Bis(1,4-di-tert-butyl-1,3-diazadienyl)cobalt and Alkylamine Precursors.* Chemistry of Materials, 2017. **29**(17): p. 7458-7466.

12. De Fazio, D., Purdie, D. G., Ott, A. K., Braeuninger-Weimer, P., Khodkov, T., Goossens, S., Taniguchi, T., Watanabe, K., Livreri, P., Koppens, F. H. L., Hofmann, S., Goykhman, I., Ferrari, A. C., Lombardo, A., *High-Mobility, Wet-Transferred Graphene Grown by Chemical Vapor Deposition.* ACS Nano, 2019. **13**(8): p. 8926-8935.

13. Binnig, G., C.F. Quate, and C. Gerber, *Atomic Force Microscope.* Physical Review Letters, 1986. **56**(9): p. 930-933.

14. *Chapter 2 X-ray probes for surface analysis (XPS or ESCA)*, in *Pergamon Materials Series*, J.W. Martin, Editor. 2003, Pergamon. p. 21-38.

15. Lee, H.-L. and N.T. Flynn, *X-RAY PHOTOELECTRON SPECTROSCOPY*, in *Handbook of Applied Solid State Spectroscopy*, D.R. Vij, Editor. 2006, Springer US: Boston, MA. p. 485-507.

16. Kumar, A., H.A. Biebuyck, and G.M. Whitesides, *Patterning Self-Assembled Monolayers: Applications in Materials Science.* Langmuir, 1994. **10**(5): p. 1498-1511.

17. Gooding, J.J., Mearns, F., Yang, W., Liu, J., *Self-Assembled Monolayers into the 21st Century: Recent Advances and Applications.* Electroanalysis, 2003. **15**(2): p. 81-96.

18. Chaki, N.K. and K. Vijayamohanan, *Self-assembled monolayers as a tunable platform for biosensor applications.* Biosensors and Bioelectronics, 2002. **17**(1): p. 1-12.

19. Chen, R., Kim, H., McIntyre, P. C., Bent, S. F., *Investigation of Self-Assembled Monolayer Resists for Hafnium Dioxide Atomic Layer Deposition.* Chemistry of Materials, 2005. **17**(3): p. 536-544.

20. Hild, R., David, C., Müller, H. U., Völkel, B., Kayser, D. R., Grunze, M., *Formation and Characterization of Self-assembled Monolayers of Octadecyltrimethoxysilane on Chromium: Application in Low-Energy Electron Lithography.* Langmuir, 1998. **14**(2): p. 342-346.

21. Caro, A.M., Armini, S., Richard, O., Maes, G., Borghs, G., Whelan, C. M., Travaly, Y., *Bottom-Up Engineering of Subnanometer Copper Diffusion Barriers Using NH2-Derived Self-Assembled Monolayers.* Advanced Functional Materials, 2010. **20**(7): p. 1125-1131.

22. Crowe, L.L. and L.M. Tolbert, *Silica Passivation Efficiency Monitored By a Surface-Bound Fluorescent Dye.* Langmuir, 2008. **24**(16): p. 8541-8546.

23. Zakir, M., Ashraf, U., Tian, T., Han, A., Qiao, W., Jin, X., Zhang, M., Tsoi, J., Matinlinna, J., *The Role of Silane Coupling Agents and Universal Primers in Durable Adhesion to Dental Restorative Materials - a Review.* Current Oral Health Reports, 2016.